International Conference on Mathematics, Computational Methods & Reactor Physics (M&C 2009)
Saratoga Springs, New York, May 3-7, 2009, on CD-ROM, American Nuclear Society, LaGrange Park, IL (2009)

COMPARISON OF MCNP AND WIMS-AECL/RFSP CALCULATIONS AGAINST CRITICAL HEAVY WATER EXPERIMENTS IN ZED-2 WITH CANFLEX-LVRF AND CANFLEX-LEU FUELS

Blair P. Bromley, David G. Watts, Jeremy Pencer, Michael Zeller, and Yousif Dweiri
Atomic Energy of Canada Limited, Chalk River Laboratories
Station 68, 1 Plant Road, Chalk River, ON, Canada, K0J 1J0
bromleyb@aecl.ca

ABSTRACT

This paper summarizes calculations of MCNP5 and WIMS-AECL/RFSP compared against measurements in coolant void substitution experiments in the ZED-2 critical facility with CANFLEX®-LEU/RU (Low Enriched Uranium, Recovered Uranium) reference fuels and CANFLEX-LVRF (Low Void Reactivity Fuel) test fuel, and H_2O/air coolants. Both codes are tested for the prediction of the change in reactivity with complete voiding of all fuel channels, and that for a checkerboard voiding pattern. Understanding these phenomena is important for the ACR-1000® reactor. Comparisons are also made for the prediction of the axial and radial neutron flux distributions, as measured by copper foil activation. The experimental data for these comparisons were obtained from critical mixed lattice / substitution experiments in AECL's ZED-2 critical facility using CANFLEX-LEU/RU and CANFLEX-LVRF fuel in a 24-cm square lattice pitch at 25°C. Substitution analyses were performed to isolate the properties (buckling, bare critical lattice dimensions) of the CANFLEX-LVRF fuel. This data was then used to further test the lattice physics codes. These comparisons establish biases/uncertainties and errors in the calculation of k_{eff}, coolant void reactivity, checkerboard coolant void reactivity, and flux distributions. Results show small to modest biases in void reactivity and very good agreement for flux distributions. The importance of boundary conditions and the modeling of unmoderated fuel in the critical experiments are demonstrated. This comparison study provides data that supports code validation and gives good confidence in the reactor physics tools used in the design and safety analysis of the ACR-1000 reactor.

Key Words: MCNP, WIMS-AECL, RFSP, ZED-2, Measurements

CANFLEX® (CANDU FLEXible Fueling) is a registered trademark of AECL and the Korea Atomic Energy Research Institute.
ACR-1000® (Advanced CANDU® Reactor) is a registered trademark of AECL.

1. INTRODUCTION

Mixed lattice / substitution experiments were performed in AECL's ZED-2 heavy-water moderator critical facility [1], to provide data to quantify the accuracy of reactor physics codes that are being used in the analysis of heavy-water reactors [2]. Two key reactor physics phenomena [2] were studied: Coolant-Density-Change-Induced Reactivity, and Flux Distribution in Space and Time. Critical moderator heights and copper foil activation rate distributions were measured in mixed-lattice experiments with 52 fuel channels in a 24.0-cm square lattice pitch with air and light water (H_2O) coolants, and also a checkerboard pattern of air and H_2O coolants. The central twelve channels of the test lattice contained primarily CANFLEX-LVRF (Low Void Reactivity Fuel) fuel, while the surrounding 24 channels contained CANFLEX-LEU (Low Enriched Uranium), and the outer 16 channels a mix of CANFLEX-LEU and CANFLEX-RU (Recovered Uranium).

The effects of the coolant density and coolant pattern on the core reactivity and the normalized flux distributions were inferred by the measurements of the critical moderator height and normalized copper foil activation rate distributions. These data were used to check the reactivity calculations (k_{eff}) and flux distributions computed by MCNP [3] and WIMS-AECL/RFSP [2], [4], [5], [6]. A substitution analysis was also performed to isolate the critical bare core dimensions and bucklings of the CANFLEX-LVRF fuel. This data was used subsequently for determining the accuracy of both code sets, along with WIMS-AECL in stand-alone calculations.

For the stochastic calculations, MCNP5 Version 1.30 [3] was used in conjunction with a nuclear data library based on ENDF/B-VI, Release 8 [7]. For the deterministic calculations, RFSP Version 3-04 [2], [5] was used in conjunction with WIMS-AECL Version 3.1 [4]. The nuclear data library for WIMS-AECL was based mainly on data obtained from ENDF/B-VI Release 5 [4], with supplementary data for dysprosium and other burnable neutron absorbers based on ENDF/B-VI Release 7 [4].

The ACR-1000 reactor [2] uses a 43-element fuel bundle design with low enriched uranium, and a central neutron absorber pin containing dysprosium and gadolinium. The ACR-1000 has a core design with a 24-cm square lattice pitch, and uses light water coolant. The CANFLEX fuels also involve the use of a 43-element fuel bundle, with enriched uranium, and in the CANFLEX-LVRF, a central neutron absorber pin containing dysprosium, which is similar in design to the fuels to be used in the ACR-1000. Thus, the results of the comparisons between MCNP, WIMS-AECL and RFSP calculations for these experiments involving CANFLEX-LEU/RU and CANFLEX-LVRF in a 24-cm square pitch lattice with both H_2O and air coolants provide relevant data that can be used to support the reactor physics toolset validation program for the ACR-1000 [2].

2. EXPERIMENTS

From Fig. 1, the 52-channel, square lattice arrangement and coordinate system in the ZED-2 critical substitution experiments with CANFLEX-LVRF and CANFLEX-LEU can be seen. Further details on the ZED-2 critical facility can be found in References [1] and [8]. The lattice pitch was 24 cm square. The central 12 channels (the substitution region) each contained a stack of 3 CANFLEX-LVRF bundles, and 2 CANFLEX-LEU bundles. The surrounding 24 channels each contained five CANFLEX-LEU bundles, while the outer 16 channels contained 4 CANFLEX-LEU bundles and 1 CANFLEX-RU bundle. This places the CANFLEX-LEU and CANFLEX-RU in regions of lower neutron importance. All channels (pressure tube and calandria tube) were made of aluminum with CANDU-type dimensions, as shown in Fig. 2.

2.1. Test Fuels

The test fuels were variations of the 0.5-m long, 43-element CANFLEX fuel bundle design [9], [10] (see Fig. 2). CANFLEX-LEU is made with slightly enriched uranium oxide (approximately 0.95 wt% ^{235}U/U), whereas CANFLEX-RU is made from recovered light water reactor (LWR) fuel, and is very similar to CANFLEX-LEU in terms of enrichment. CANFLEX-LVRF uses a slightly higher enrichment (approximately 1.0 wt% ^{235}U/U) for the outer 42 pins, and the central pin contains dysprosia in natural uranium oxide.

2.2. Activation Foils

Over fifteen critical experiments were performed with different coolant patterns (air/checkerboard/H_2O), and different arrangements of copper activation foils in the lattice. Up to four different foil arrangements were tested for each coolant pattern, along with a critical measurement without foils. One sample foil arrangement is shown in Fig. 1. Each of the copper activation foils was attached to an aluminum backing on a zirconium wire stringer suspended from a steel beam above the top of the reactor. The copper foils were positioned at regular 10-cm axial and 24-cm radial intervals in the high-flux zones (lattice radial positions K2W, K2E (Fig. 1) for axial foils, axial positions z=60 cm to 110 cm for radial foils).

2.3. Operational Conditions

Over the course of the experiments, the moderator purity decreased from approximately 99.125 wt%D_2O to 99.104 wt%D_2O. The moderator/coolant temperature was held relatively constant, ranging only slightly from 25.2°C to 25.7°C. The critical height varied from 154.2 cm for the air-cooled lattice to 221.5 cm for the H_2O-cooled lattice (shown in Table I). In the ZED-2 reactor, there are bottom D_2O and graphite axial reflectors. The bottom of the fuel is approximately 15 cm above the aluminum calandria of ZED-2. The length of the five-bundle fuel string is approximately 250 cm. Thus, the exposed amount of unmoderated fuel varied from approximately 2.2 bundles (air-cooled case) to 0.9 bundles (H_2O-cooled case).

2.4. Measurement Uncertainties and k_{eff} Sensitivities

The heavy water moderator purity was measured with an uncertainty of ±0.005 wt%. The digital thermometers used in the experiment had an absolute uncertainty of ±0.2 ^{o}C. The uncertainty in the measured critical moderator height was ±0.2 cm. The uncertainties in these parameters propagate into the uncertainty in the value of k_{eff} calculated by MCNP and WIMS-AECL/RFSP for each simulated experiment. The sensitivity of k_{eff} to D_2O moderator purity for these particular models was found to vary from approximately 15 mk/wt%D_2O (air-cooled) to 25 mk/wt%D_2O (H_2O-cooled), (1 mk = 100 pcm = 0.001 Δk/k). This resulted in an uncertainty in k_{eff} of ±0.13 mk or less due to the uncertainty in moderator purity. The sensitivity of k_{eff} to D_2O moderator height was found to range approximately from 0.4 mk/cm (H_2O-cooled) to 1.1 mk/cm (air-cooled). Since the uncertainty in the D_2O moderator height is ±0.20 cm, these yield uncertainties in k_{eff} of ±0.22 mk and ±0.08 mk for the air-cooled and H_2O-cooled cases, respectively. Both WIMS-AECL/RFSP and MCNP showed similar sensitivities. The statistical MCNP uncertainties in k_{eff} ranged from approximately ±0.03 mk to ±0.04 mk (for 300 million history tallied runs) to approximately ±0.09 mk to ±0.11 mk (for 30 million history untallied runs). Thus, the combined uncertainties in k_{eff} ranged from approximately ±0.2 mk for the H_2O-cooled runs to ±0.3 mk for air-cooled runs. By combining the results from similar repeated experiments, these uncertainties can be reduced to less than ±0.15 mk.

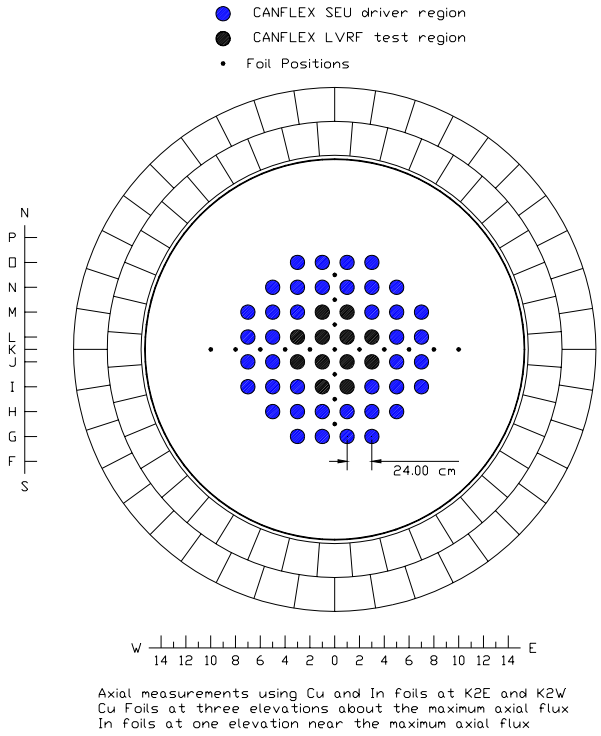

Figure 1. Top view of ZED-2 lattice with foil positions.

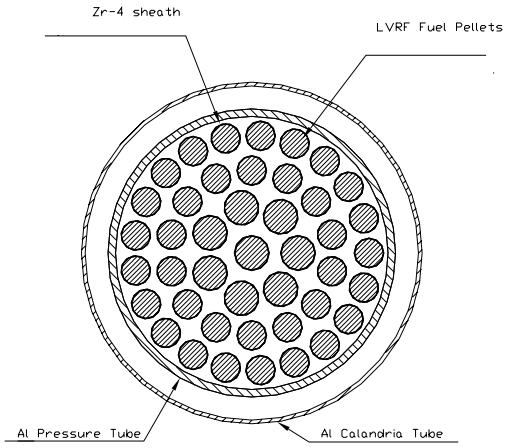

Figure 2. Section view of CANFLEX-LVRF bundle.

Table I. Sample reactor core conditions for selected substitution experiments

Case #	Coolant	Moderator Purity (wt% D_2O)	Core Temperature (°C)	Critical Height (cm)	Approx. # Unmoderated Bundles
7	air	99.125	25.16	154.25	2.2
14	CHKB	99.119	25.57	173.93	1.8
21	H_2O	99.104	25.55	221.51	0.9

3. CODES AND COMPUTATIONAL MODELS

3.1. MCNP5

The MCNP5 models used were an approximation of the actual experimental set-up. The model included the fuel bundles, aluminum fuel channels, the bottom and radial D_2O reflector, the aluminum calandria tank, the bottom and radial graphite reflector, the outer neutron shielding, steel hanger rods, various air gaps, etc. The unmoderated fuel above the moderator level was modeled explicitly.

Detailed models of the 43-element fuel bundles with cylindrical fuel elements were created for the CANFLEX-LEU, CANFLEX-RU, and CANFLEX-LVRF fuel types. The Al-backed Cu foil and Zr-wire stringers were also modeled for these experiments with high precision, using

rectangular prisms. Since their orientations can vary from location to location (and from time to time), the orientation of the aluminum backers alternated orientations from N-S to W-E.

The MCNP models were set up to ensure the correct material compositions and that the material temperatures closely matched those of the experiment. Since the MCNP libraries are generated at fixed temperatures that may differ from those of the experiment, material properties for input were created using mixes of library data at different fixed temperatures. The approach was the same as that described in [9].

These experiments were modeled in MCNP5 using up to 30 million neutron histories for the non-foil (untallied) experiments and 300 million neutron histories for the foil (tallied) experiments. This ensured that the statistical uncertainty in the calculation of k_{eff} was less than ±0.1 mk. Extra histories were required for modeling the foil experiments in order to obtain low statistical uncertainties in the simulated foil activation rates.

3.2. WIMS-AECL 3.1

WIMS-AECL 3.1 [4] is a two-dimensional lattice physics code that solves the integral neutron transport equation using collision probabilities, and is used in conjunction with an 89-group nuclear data library based on ENDF/B-VI.5 and ENDF/B-VI.7. WIMS-AECL is used to generate homogenized two-group cross sections that are used in the RFSP 3-D diffusion model of the ZED-2 reactor. Latest code enhancements incorporated in WIMS-AECL 3.1 include a more refined geometric discretization and numerical solution, distributed resonance self-shielding, and a multi-cell (colorset) capability that permits a more accurate representation of the environment for a given lattice cell. These features are particularly important when modeling scenarios with checkerboard coolant (in a postulated loss-of-coolant accident), or at the core/reflector interface, where there is a change in the neutron energy spectrum.

A variety of single-cell and WIMS-AECL multi-cell models was used to determine the lattice physics properties. Single-cell models were used for fuel channels surrounded by identical fuel and coolant (eg. the central four CANFLEX-LVRF/LEU channels), whereas 2×5 multi-cell models (with six fuel cells and four reflector cells) were used to obtain the properties of the outer 48 channels. In situations with checkerboard cooling, the central four channels were modeled with 2×1 multi-cell models. The single-cell and 2×1 multi-cell model used periodic boundary conditions, with a critical buckling search using the solution of the B1 equations with Benoist diffusion coefficients. The 2×5 multi-cell models used a combination of reflecting, periodic, and vacuum boundary conditions permitting leakage. Simplified representations of these models are shown in Fig. 3. The two-group properties for the materials outside the reactor core (D_2O reflector, graphite reflector, aluminum calandria, etc.) were determined in a more approximate way from a simple super-cell model with a single annular lattice cell channel surrounded by annuli of these materials. The thickness of these material annuli was made to preserve the ratio of the area of the materials in the reactor to the area of the reactor core (52 lattice cells).

The data processing code system WIMS Utilities [5] was used to execute WIMS-AECL and to process the 89-group output flux and reaction rate data from the WIMS-AECL calculations to

create homogenized two-group cross section data that would be used in the RFSP models of the ZED-2 experiments.

WIMS-AECL was also used in a "stand-alone" mode with an input buckling imposed upon the leakage model in single-cell calculations to evaluate k_{eff}, and thereby provide a direct accuracy determination of WIMS-AECL using buckling data derived from the substitution experiments.

In the standard WIMS-AECL approach, the multi-group two-dimensional transport equation is first solved without leakage to get the infinite lattice eigenvalue (k_{inf}) and the heterogeneous flux solution. Then, the energy spectrum of the homogenized lattice is adjusted to include leakage according to the input buckling, such as to produce $k_{eff.}$ [4].

3.3. RFSP 3-04

The RFSP code [6] solves the three-dimensional, two-group neutron diffusion equations using finite difference methods in Cartesian coordinates (x-y-z), and is used to determine reactivity levels and changes, and flux and power distributions. The WIMS-AECL models described in the previous section were used to generate the two-group homogenized cross section data used for the various materials in the RFSP model of ZED-2. The RFSP models of the ZED-2 experiments were more approximate that those set up with MCNP. A mesh spacing of 12 cm was used for the core region (2 meshes per lattice cell), while a range of other meshes (from 3 cm to 14 cm) was used to approximate the circular boundaries of the radial D_2O reflector, calandria, and radial graphite reflector. The RFSP model of the ZED-2 reactor extended to the physical boundary of the radial and bottom graphite reflectors, with vacuum boundary conditions imposed.

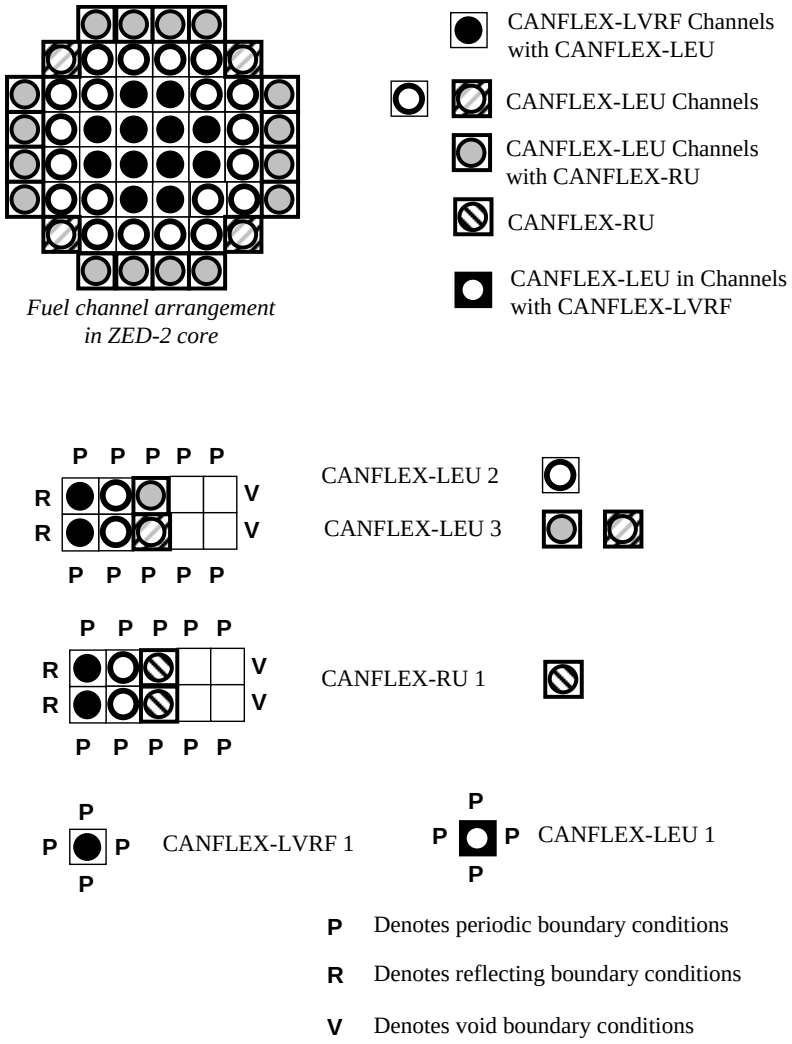

Figure 3. WIMS-AECL 5×2 multi-cell model configurations.

The non-uniform mesh spacing in the axial direction ranged from approximately 1.5 cm to 10 cm. In the upper axial direction, the RFSP model extended to the top of the moderated fuel. Above the moderator level either a vacuum boundary condition was imposed, or an extrapolation distance based on the experimentally measured flux distribution was used. The latter boundary condition accounted for the reactivity effect of the unmoderated fuel in a very approximate way. As an alternative approach, an attempt was also made to model the unmoderated fuel explicitly in RFSP, although it was recognized that such an approach would be testing the limits of the diffusion theory. Two-group homogenized cross section data for the unmoderated fuel was obtained by using an (r-z) DRAGON neutron transport model [11] of a single channel including the bottom graphite and D_2O reflector, and the moderated and unmoderated fuel. The 89-group cross section data for the DRAGON model was obtained from single-cell WIMS-AECL models, making use of what is known as the side-step method [11].

The copper activation rate distributions were obtained by combining the two-group fluxes computed by RFSP with effective two-group copper cross sections determined approximately from single-cell WIMS-AECL models. Two-group copper activation rates were computed in WIMS-AECL models at cell positions corresponding to their positioning in the experiment (e.g. the lattice cell corners) and then normalized by the lattice-cell-average two-group fluxes. This approach was essentially a simple form of flux reconstruction.

4. RESULTS

In total, three non-foil (untallied) and twelve foil (tallied) MCNP and WIMS-AECL/RFSP simulations were completed, corresponding to the ZED-2 critical experiments. In each of the MCNP runs, the first 100 cycles were dropped for tally convergence, and the subsequent 3000 cycles were used for tally (and k_{eff}) convergence. In the tallied cases, 10^5 histories per cycle were used, while, in the untallied cases, 10^4 histories per cycle were used, giving totals of 30×10^6 histories and 300×10^6 histories per untallied and tallied run, respectively. The tallies used were cellular flux tallies. They were tallied on both the thin circular foil-cells, and also on the cylindrical D_2O-filled cells surrounding the aluminum backers, as a method of reducing statistical uncertainties.

4.1 Reactivity Calculations

Reactivity calculations for the various mixed-lattice substitution experiments and model types are shown in Table II. The k_{eff} values were those averaged over all the experiments that had nearly identical operational conditions, and only differed in arrangement of activation foils. The k_{eff} calculations for MCNP were approximately 7 mk to 10 mk below unity, with a coolant void reactivity (CVR) bias (ΔCVR) of approximately +3.3 mk, and a checkerboard CVR bias (ΔCBCVR) of approximately +2.1 mk. The k_{eff} calculations for the RFSP simulations tended to be higher, ranging from 5 mk below unity to 3 mk above unity, depending on the coolant conditions and the treatment of the upper axial boundary condition. The differences between the RFSP and MCNP k_{eff}s are explained by several factors including spatial and energy group discretization, homogenization, and nuclear data. In general, these differences should lead to systematic errors in the calculation of k_{eff}. The uncertainties in CVR and CBCVR bias ($\pm$0.2 mk) are the propagated uncertainties due to experimental uncertainties in moderator purity and moderator height.

Of more interest is the change in reactivity with coolant density, as shown in the calculations of ΔCVR and ΔCBCVR. The CVR bias for RFSP was found to range from –1.6 mk to +2.4 mk, depending on the treatment of the boundary condition at the moderator surface. The checkerboard CVR bias was found to range from +1.3 mk to +4.4 mk. Unlike the MCNP calculations, the RFSP results showed a larger checkerboard CVR bias, but this is likely explained by the approximate approaches for modeling the reactivity effect of the unmoderated fuel. The RFSP simulations which explicitly model the unmoderated fuel using diffusion theory as a rough approximation show a reactivity change of +2.5 mk to +6.5 mk relative to the RFSP models where a simple vacuum boundary condition is imposed at the top of the moderator level.

However, it was observed that achieving good convergence in the flux distribution in this particular case was difficult. In the air-cooled experiments, more than two bundles are above the moderator level.

Table II. Reactivity Calculations for Substitution Experiments

Model	k_{eff}			ΔCVR (mk)	ΔCBCVR (mk)	Uncertainty (mk)
	Air	Ckbd	H_2O			
MCNP	0.99344	0.99229	0.99019	+3.3	+2.1	±0.2
RFSP - Vacuum BC	0.99455	0.99746	0.99615	-1.6	+1.3	±0.2
RFSP - Exp. BC	0.99648	0.99944	0.99683	-0.4	+2.6	±0.2
RFSP + Unmod Fuel	1.00108	1.00307	0.99864	+2.4	+4.4	±0.2

4.2 Neutron Flux Distributions

Results for copper foil activation rate distributions as computed by MCNP and WIMS-AECL/RFSP are shown for three sample cases (air-cooled, checkerboard, H_2O-cooled) in Fig. 4 to Fig. 9. For simplicity of comparison, both the experimental and calculated activation data were normalized by one of the high-flux data points in radial position K0. The WIMS-AECL/RFSP calculations were based on those obtained using the experimentally based extrapolation distance. The agreement between MCNP and the experimental measurements was excellent for both axial and radial distributions, with local percentage errors of usually less than 2%, and a Root-Mean-Square (RMS) error of less than 1%. The agreement between WIMS-AECL/RFSP and the experiment was also quite good, particularly in the H_2O-cooled case. The RMS error was usually less than 2.5%. The largest local discrepancies were found in the checkerboard case, and in all cases near the core/reflector interface, and near the top of the core. This was not surprising since in these regions there are significant changes in the neutron energy spectrum. The local % differences typically ranged from –3% to +3% in the radial direction and +2% to –5% in the axial direction, becoming more negative near the top of the core. The discrepancies for the WIMS-AECL/RFSP results near the core/reflector interface can also be explained in part by the approximate method of the flux reconstruction method used to convert the two-group fluxes by RFSP into local copper activation rates. Considering that the experimental activation data has an uncertainty of typically ±1% due to counting statistics and asymmetry of positioning in the core, this level of agreement with WIMS-AECL/RFSP was quite good.

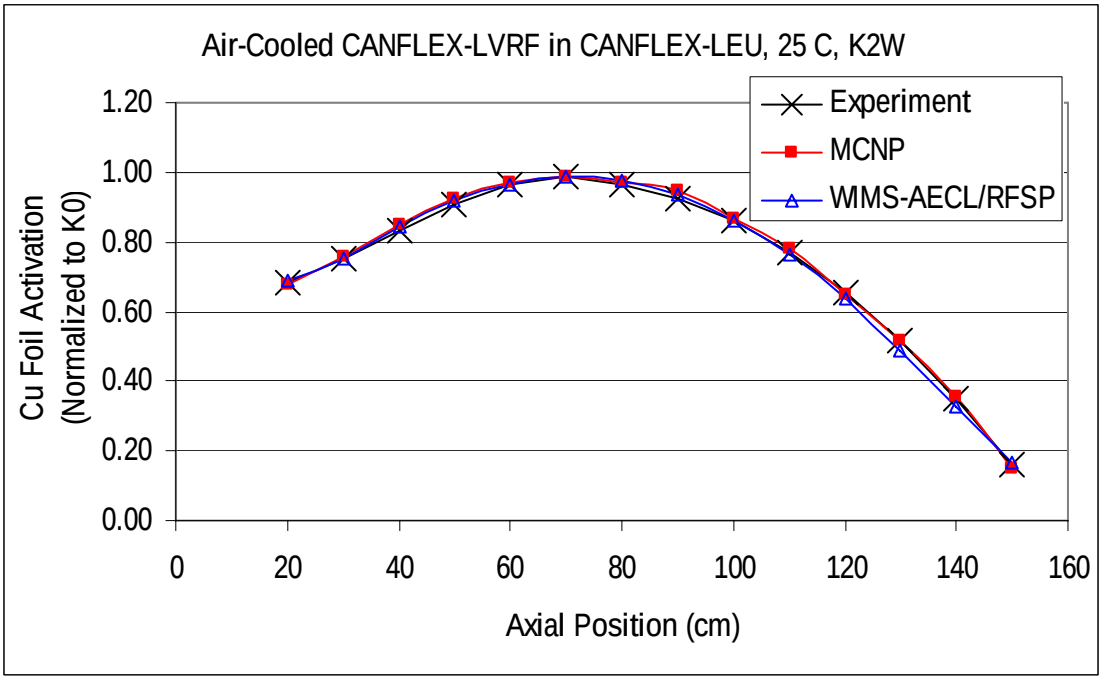

Figure 4. Axial flux distributions for air-cooled lattice.

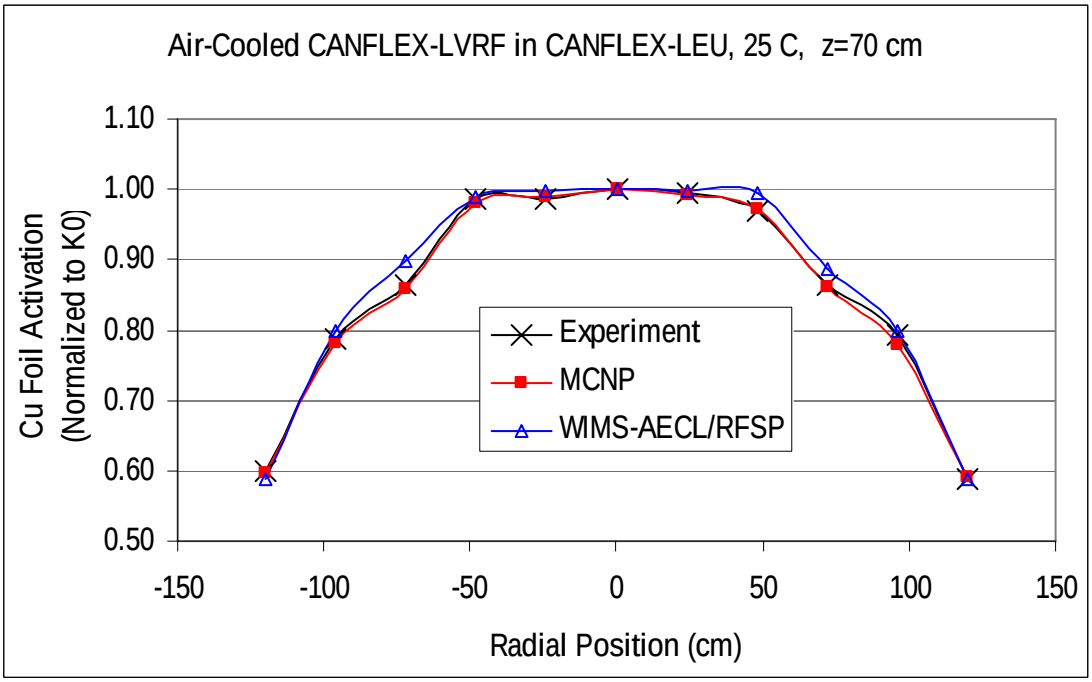

Figure 5. Radial flux distributions for air-cooled lattice.

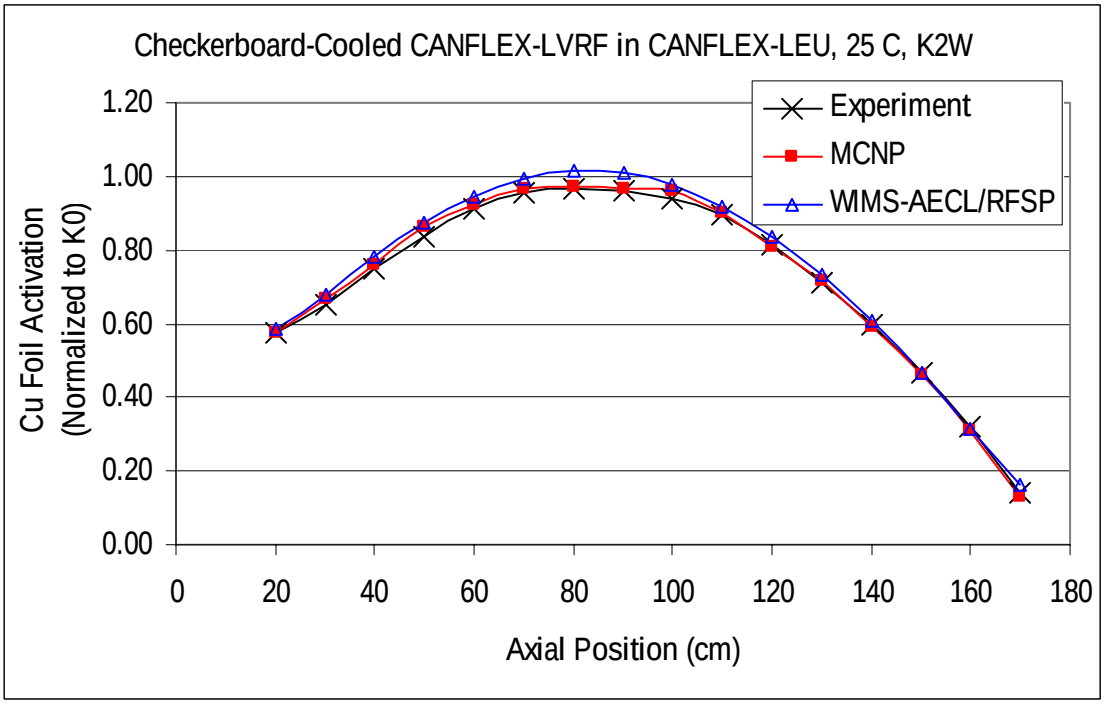

Figure 6. Axial flux distributions for checkerboard-cooled lattice.

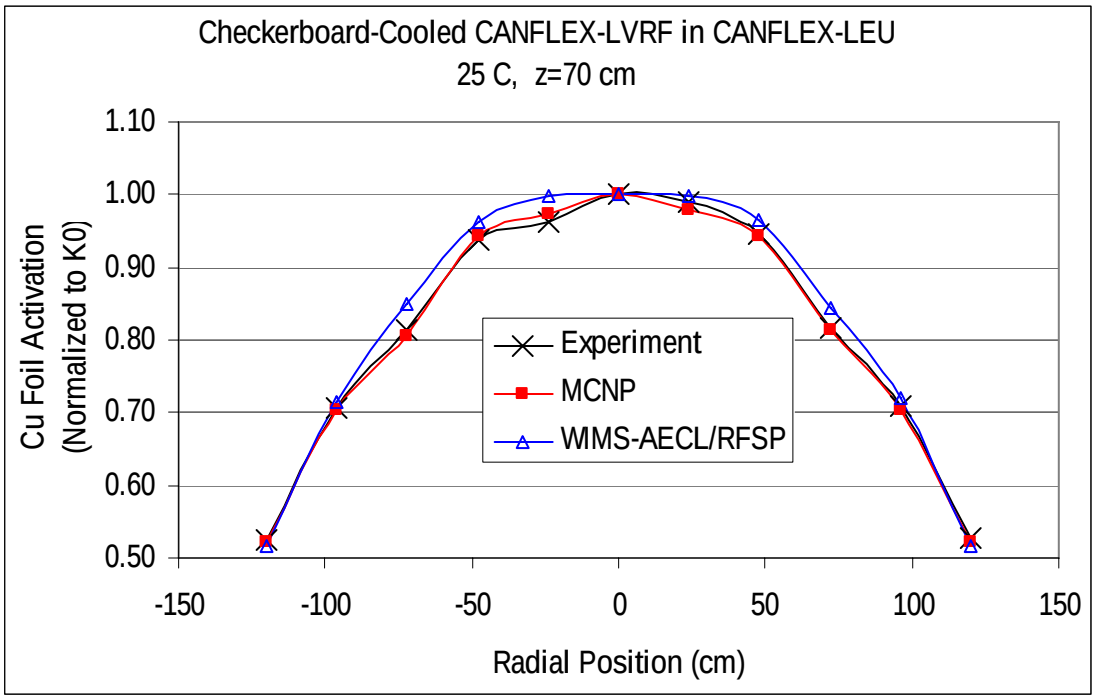

Figure 7. Radial flux distributions for checkerboard-cooled lattice.

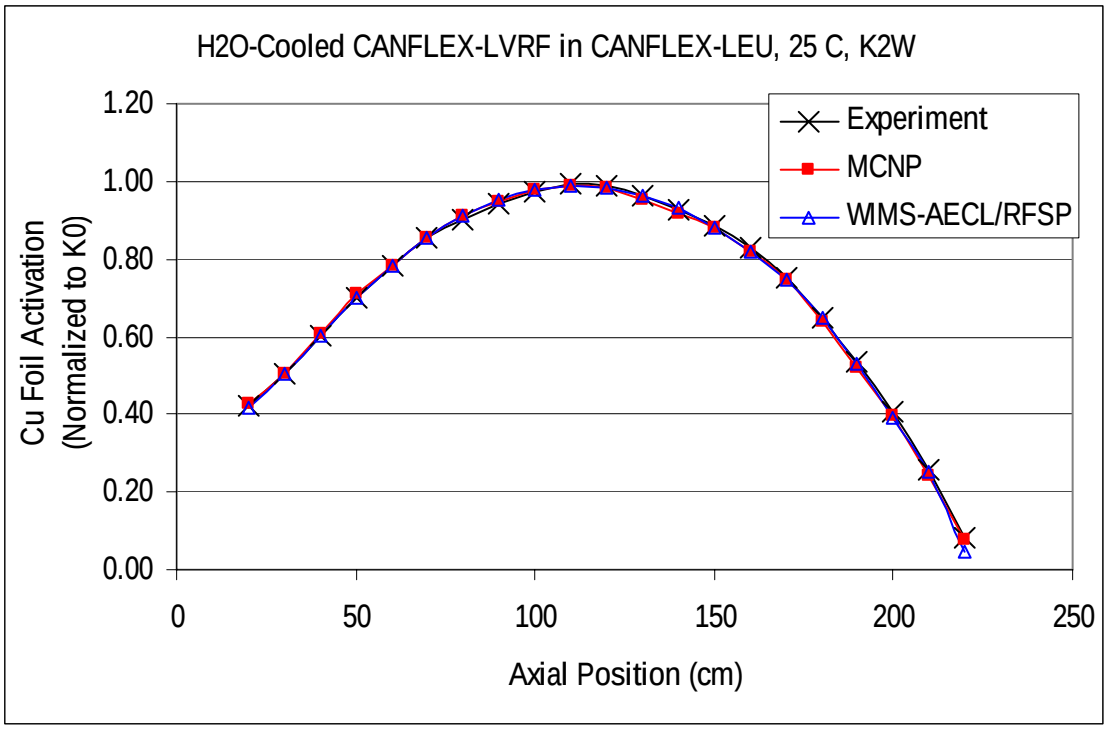

Figure 8. Axial flux distributions for H_2O-cooled lattice.

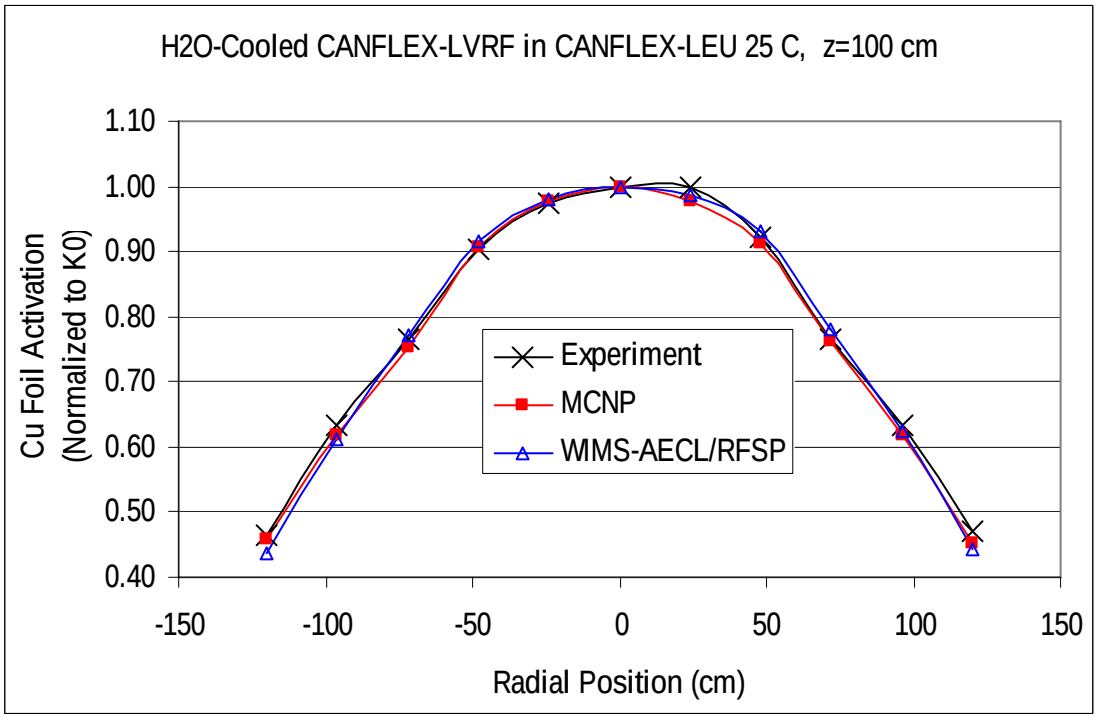

Figure 9. Radial flux distributions for H_2O-cooled lattice.

4.3 Bare Core CANFLEX-LVRF Simulations

The experiments performed with CANFLEX-LVRF were mixed-lattice substitution experiments. Simulations of these experiments with MCNP and WIMS-AECL/RFSP give an indication of the biases in k_{eff} and void reactivity for a mixed lattice; however, what is of particular interest is to quantify the biases for the test fuel in the substituted region (CANFLEX-LVRF) alone. The properties of the reference lattice are well understood, and were shown in previous studies [9], [12].

To isolate the properties of the CANFLEX-LVRF from the CANFLEX-LEU/RU, substitution analyses were performed making use of the methods described in [12] and [13], and the dimensions and bucklings of bare critical lattices of air-cooled, and H_2O-cooled CANFLEX-LVRF were determined and shown in Table III. Bare lattices of varying sizes were found, with heights corresponding to four, five and ten bundle lengths. As can be seen, there is a slight increase in the total critical buckling with increased core height, which is mainly due to reduced leakage from axial neutron streaming. If bare-lattice experiments with H_2O-cooled CANFLEX-LVRF were to be set up, a minimum of 234 channels with five bundles per channel would be required. Lattice properties determined from substitution experiments have inherently larger uncertainties, which can be reduced by repeated experiments.

The critical dimensions were then used in MCNP and WIMS-AECL/RFSP simulations of bare cores of CANFLEX-LVRF to compute k_{eff}. Single-cell WIMS-AECL models with a critical buckling search were used to generate the two-group data for the RFSP models since all lattice cells were identical. The RFSP model of the bare core approximated the shape of a circle, but used an integer number of square lattice cells [6]; this approximation works better for larger radius cores. The derived bucklings were used directly in stand-alone WIMS-AECL 89-group calculations for k_{eff}.

Results of k_{eff} calculations for the various bare cores of CANFLEX-LVRF are shown in Table IV. MCNP results are the same for all cores, and range from –4 mk to –7 mk below unity with an uncertainty of approximately ±0.3 mk. The WIMS-AECL/RFSP calculations also had k_{eff} biases that ranged from –4 mk to –7 mk; however, the biases tended to become more negative with core height. The differences between WIMS-AECL/RFSP and MCNP are attributed to differences in spatial, energy and angular approximations in the neutron transport calculations, along with slight differences in the nuclear data libraries. The WIMS-AECL calculations of k_{eff} were 1.5 mk to 3 mk below the values computed by WIMS-AECL/RFSP, and showed a similar trend with core height. The leakage model was anisotropic, with axial leakage being enhanced by neutron streaming. The differences between the stand-alone WIMS-AECL results and the WIMS-AECL/RFSP calculations can be explained by homogenization effects, the fact that the two-group data generated by WIMS-AECL used an equal-component critical buckling search, and the approximate representation of a circular core with RFSP.

The k_{eff} calculations for the bare core CANFLEX-LVRF were used to compute the biases in the coolant void reactivity (ΔCVR) and are shown for the various critical core dimensions and calculation methods in Table V. The MCNP results were independent of core height, with a value of approximately +2.7 mk. This value is less than that for the mixed lattice (+3.3 mk),

indicating that a pure lattice of CANFLEX-LEU may have a slightly higher CVR bias. This was confirmed by the results found in [9]. The WIMS-AECL/RFSP results varied from –0.3 mk to +0.1 mk, while the stand-alone WIMS-AECL results varied from +0.3 mk to +0.7 mk. The WIMS-AECL calculations have a slightly larger uncertainty in CVR bias (±0.7 mk) due to the propagation of the uncertainty in buckling. Both the MCNP and WIMS-AECL/RFSP results had an uncertainty of approximately ±0.4 mk, which is due to the uncertainty in the results from substitution analysis. The WIMS-AECL/RFSP and stand-alone WIMS-AECL results for the bare lattice are equal within their uncertainties. Differences occur due to spatial and energy homogenization. The WIMS-AECL/RFSP and stand-alone WIMS-AECL results CVR bias for the CANFLEX-LVRF are approximately 2 mk to 3 mk less than the results found with MCNP.

Table III. CANFLEX-LVRF bare lattice critical dimensions and bucklings

Coolant	Critical Dimensions		Buckling			
	H_c (cm)	R_c (cm)	B^2_z (m^{-2})	B^2_r (m^{-2})	B^2 (m^{-2})	$\pm\delta B^2$ (m^{-2})
Air	198.04	252.30	2.369	0.882	3.250	0.015
Air	247.55	178.34	1.535	1.759	3.294	0.015
Air	495.10	136.78	0.395	2.971	3.366	0.015
H_2O	198.04	366.50	2.390	0.422	2.812	0.013
H_2O	247.55	207.00	1.547	1.321	2.868	0.013
H_2O	495.10	148.62	0.393	2.539	2.932	0.013

Table IV. k_{eff} calculations for CANFLEX-LVRF bare lattice

Coolant	Critical Dimensions		MCNP		WIMS-AECL/RFSP		WIMS-AECL	
	H_c (cm)	R_c (cm)	keff	±δkeff	keff	±δkeff	keff	±δkeff
Air	198.04	252.30	0.99584	±0.00035	0.99612	±0.00035	0.99334	±0.00058
Air	247.55	178.34	0.99584	±0.00036	0.99503	±0.00036	0.99300	±0.00059
Air	495.10	136.78	0.99584	±0.00037	0.99346	±0.00037	0.99217	±0.00058
H_2O	198.04	366.50	0.99320	±0.00025	0.99598	±0.00025	0.99282	±0.00039
H_2O	247.55	207.00	0.99320	±0.00026	0.99501	±0.00026	0.99230	±0.00039
H_2O	495.10	148.62	0.99320	±0.00027	0.99377	±0.00027	0.99184	±0.00039

Table V. CVR bias calculations for CANFLEX-LVRF bare lattice

	MCNP		WIMS-AECL/RFSP		WIMS-AECL	
Hc (cm)	ΔCVR (mk)	±δCVR (mk)	ΔCVR (mk)	±δCVR (mk)	ΔCVR (mk)	±δCVR (mk)
198.04	+2.7	±0.4	+0.1	±0.4	+0.5	±0.7
247.55	+2.7	±0.4	+0.0	±0.4	+0.7	±0.7
495.10	+2.7	±0.4	-0.3	±0.4	+0.3	±0.7

4.4 Relevance of Calculation Results for Code Validation for ACR-1000

The experiments described in Section 3 and the calculation results shown in Sections 4.1, 4.2, and 4.3 demonstrate the quantification of the accuracy of WIMS-AECL, RFSP, and MCNP for predicting the physics behavior in ZED-2 experiments with ACR-type lattices. These results can be used for the validation of these codes for application to the ACR-1000, and are part of the overall validation plan for the physics toolset for ACR-1000 [2]. The code biases and uncertainties in the coolant void reactivity are those for ZED-2 experiments, and they can be extended to the design and operational conditions of the ACR-1000 through the use of TSUNAMI analyses, as discussed in more detail in [2] and [14].

5. CONCLUSIONS

This paper summarizes the sample calculations of MCNP5 and WIMS-AECL/RFSP compared against measurements in coolant void substitution critical experiments in the ZED-2 critical facility with CANFLEX®-LEU/RU reference fuels and CANFLEX-LVRF test fuel. Mixed lattice cores with H_2O coolant, air coolant, and a checkerboard arrangement of H_2O-cooled and air-cooled channels were tested.

Calculations for mixed lattices of CANFLEX-LVRF and CANFLEX-LEU/RU show k_{eff} biases of approximately –7 mk to –10 mk for MCNP with a CVR bias of approximately +3.3 mk, and a checkerboard CVR bias of approximately +2.1 mk, whereas the WIMS-AECL/RFSP calculations show k_{eff} biases ranging from –6 mk to +3 mk, CVR biases ranging from –1.6 mk to +2.4 mk, and checkerboard CVR biases ranging from +1.3 mk to +4.4 mk, depending on how the upper axial boundary condition is treated. The use of adjusted moderator heights to account for the reactivity effect of the unmoderated fuel is likely to give RFSP results that are much closer to MCNP results, and this approach will be given consideration in future studies.

Plots of normalized measured and predicted copper activation distributions show excellent agreement for MCNP with RMS errors of less than 1%, and very good agreement for WIMS-AECL/RFSP with RMS errors of less than 2.5%.

Calculations for models of bare lattices of CANFLEX-LVRF using critical dimensions and bucklings derived from substitution analyses show a CVR bias of approximately +2.7 mk ±0.4 mk for MCNP, and CVR biases ranging from –0.3 mk to +0.1 mk ±0.4 mk for WIMS-AECL/RFSP, and CVR biases ranging from +0.3 mk to +0.7 mk ±0.7 mk for stand-alone WIMS-AECL calculations.

The results from this study comparing WIMS-AECL, RFSP, and MCNP calculations with measurements in critical experiments in ZED-2 with ACR-type lattices (24-cm pitch, low-enriched fuel, light water coolant) demonstrate very good agreement for the prediction of neutron flux distributions, and low biases in the prediction of coolant void reactivity. These results give good confidence in the ability of these codes to accurately model the physics of the ACR-1000.

ACKNOWLEDGMENTS

The authors gratefully acknowledge the support and assistance provided by the following staff at AECL: Fred Adams, Dan Roubtsov, Dimitar Altiparmakov, Peter Schwanke, Tony Liang, Bronwyn Hyland, Benoit Arsenault, Adriaan Buijs, Boris Shukhman, Ron Davis, Elisabeth Varin, Jim Sullivan, and Michele Kubota.

REFERENCES

1. M.B. Zeller, "Physics Experiments in the ZED-2 Reactor in Support of the Advanced CANDU Reactor," *Proceedings of 25th CNS Annual Conference,* Toronto, June 6-9 (2004).
2. B.P. Bromley et al., "Validation of MCNP and WIMS-AECL/DRAGON/RFSP for ACR-1000 Applications," *Proceedings of PHYSOR 2008*, Interlaken, Switzerland, September 14-19 (2008).
3. X-5 Monte Carlo Team, *MCNP – A General Monte Carlo N-Particle Transport Code, Version 5*, LA-UR-03-1987, Los Alamos, NM, April (2003).
4. D.V. Altiparmakov, "New Capabilities of the Lattice Code WIMS-AECL," *Proceedings of PHYSOR 2008*, Interlaken, Switzerland, September 14-19 (2008).
5. T. Liang et al., "Improvement and Qualification of WIMS Utilities," *Proceedings of 29th CNS Annual Conference*, Toronto, June 1-4 (2008).
6. W. Shen et al., "Benchmarking of WIMS-AECL/RFSP Multi-cell Methodology with MCNP for ACR-1000 Full-Core Calculations," *Proceedings of PHYSOR 2008*, Interlaken, Switzerland, September 14-19 (2008).
7. R.D. Mosteller, "ENDF/B-VII.0, ENDF/B-VI, JEFF-3.1, and JENDL-3.3 Results for the MCNP Criticality Validation Suite and Other Criticality Benchmarks," *Proceedings of PHYSOR 2008*, Interlaken, Switzerland, September 14-19 (2008).
8. IAEA, *Directory of Nuclear Reactors*, Volume V, pp. 223-224, Vienna, (1964).
9. D.G. Watts et al., "Comparison of MCNP Calculations Against Measurements in Moderator Temperature Experiments with CANFLEX-LEU in ZED-2," *Proceedings of 29th CNS Annual Conference*, Toronto, June 1-4 (2008).
10. B.P. Bromley et al., "WIMS-AECL Validation for 43-Element Bruce-B Low Void Reactivity Fuel," *Proceedings of 25th CNS Annual Conference*, Toronto, June 6-9 (2004).
11. R.S. Davis, "Qualification of DRAGON for Reactivity Device Calculations in the Industry Standard Toolset," *Proceedings of 25th CNS Annual Conference*, Toronto, June 6-9 (2004).
12. Y. Dweiri et al., "Comparison of Bare-Lattice Calculations Using MCNP Against Measurements with CANFLEX-LEU in ZED-2," *Proceedings of 29th CNS Annual Conference*, Toronto, June 1-4 (2008).
13. B.P. Bromley et al., "Development and Testing of a MCNP-Based Method for the Analysis of Substitution Experiments," *Transactions of the American Nuclear Society*, Volume 97, pp. 711-712 (2007).
14. B.T. Rearden, M.L. Williams, and J.E. Horwedel, "Advances in the TSUNAMI sensitivity and uncertainty analysis codes beyond SCALE 5," *Transactions of the American Nuclear Society*, Volume 92, pp. 760-762. (2005)